NEOPLASIA
www.neoplasia.com

Volume 18 Number 6 June 2016 pp. 329–338 329

miR-21, miR-155, miR-192, and miR-375 Deregulations Related to NF-kappaB Activation in Gastroduodenal Fluid–Induced Early Preneoplastic Lesions of Laryngeal Mucosa *In Vivo*[1]

Clarence T. Sasaki and Dimitra P. Vageli

Department of Surgery, Yale Larynx Laboratory Yale School of Medicine, New Haven, CT, USA

Abstract

Gastroduodenal refluxate found in the upper aerodigestive tract is not clinically uncommon. We recently demonstrated the neoplastic potential of gastroduodenal fluids (GDF) on hypopharyngeal mucosa, via NF-κB, using *in vitro* and *in vivo* models. Here we will explore the *in vivo* effect of GDF on laryngeal mucosa (LM) to induce early preneoplastic lesions related to NF-κB activation, along with deregulation of specific microRNA (miRNA) markers previously linked to laryngeal cancer. We used histological, immunohistochemical, automated quantitative analysis and quantitative polymerase chain reaction to examine LM from 35 C57Bl/6J mice previously treated with topical GDF against corresponding controls (4 experimental and 3 control groups; 5 mice/group). Our analysis showed that GDF produced early preneoplastic lesions in treated LM related to NF-κB activation. LM treated by acid and bile combination demonstrated significantly higher expression of the analyzed cell proliferation markers (Ki67, CK14, Np63), oncogenic p-STAT3, and changes of cell adhesion molecules (E-cadherin, -catenin) versus untreated LM or LM exposed to acid alone ($P < .0005$). Furthermore, acidic bile but not neutral bile appeared to accelerate the expression of "oncomirs" miR-21, miR-155, and miR-192 (acidic bile versus neutral bile, $P < .0001$), while reducing tumor suppressor miR-375 (acidic bile versus neutral bile, $P = .0137$), previously linked to NF-κB and laryngeal cancer. Finally, acidic bile induced reduction of miR-34a, miR-375, and miR-451a, exhibiting an inverse correlation with NF-κB activation. *SIGNIFICANCE:* Bile in combination with acid has a selective tumorigenic effect on LM, inducing deregulation of "oncomirs" and tumor suppressor miRNAs, produced by NF-κB activation with molecular and early histopathological alterations linked to neoplastic transformation. Systematic acid suppression may in part convey a protective role.

Neoplasia (2016) 18, 329–338

Introduction

Gastroesophageal reflux disease (GERD) is estimated to affect 19 million Americans, whereas its prevalence has significantly increased in the United States over the last two decades, ranging from 18.1% to 27.8% [1,2]. Furthermore, there is growing evidence that approximately 50% to 80% of patients with GERD present with mixed gastric and duodenal bile acids in their refluxate [3,4], whereas the clinical prevalence and magnitude of gastroduodenal reflux may be actually greater than it was previously reported, according to Covington et al [5]. There is further evidence that extraesophageal bile acids found in the upper aerodigestive tracts of patients are now linked to advanced

Address all correspondence to: Clarence T. Sasaki, MD, Department of Surgery, Section of Otolaryngology, Yale Larynx laboratory, Yale School of Medicine, 800 Howard Ave, 4th Floor, New Haven, CT 06519.
E-mail: clarence.sasaki@yale.edu

[1] Grant support: This study was supported in part by an Ohse Award of Yale School of Medicine and by the Virginia Alden Wright Fund.
Received 28 March 2016; Revised 11 April 2016; Accepted 22 April 2016

1476-5586
http://dx.doi.org/10.1016/j.neo.2016.04.007

inflammatory lung disease [6], whereas several observations describe a growing association of larynx cancer and reflux disease [7–9].

Constitutive activation of NF-κB has been observed in various cancers, including head and neck squamous cell carcinomas (HNSCCs) [10,11]. Its downstream oncogenic pathways that are related to combined or independent effects of inflammatory risk factors may also be crucial for the development of malignant transformation in laryngeal mucosa (LM). Altered microRNA (miRNA) profiles induced by elevated NF-κB activity play a key role in molecular dysfunctions linking inflammation to cancer [12]. We recently demonstrated the role of gastroduodenal fluid (GDF) in hypopharyngeal neoplasia through activation of the NF-κB pathway using an *in vitro* model of human hypopharyngeal normal keratinocytes [13]. Moreover, our recent findings from a novel *in vivo* model of C57Bl/6J mice [14] links NF-κB activation to early premalignant hypopharyngeal mucosal (HM) lesions, in a short period of 45 days when topically treated with GDFs, and particularly with acidic bile or deoxycholic acid (DCA), one of the active components of bile. In that study, we identified underlying molecular alterations supporting the process of malignant transformation, including markers of increased cell proliferation (Ki67, CK14, ΔNp63), epithelial mesenchymal transition (EMT) by changes of cell adhesion molecules E-cadherin and β-catenin, and activation of STAT3 oncogene.

Similar to NF-κB transcriptional factors, miRNA molecules have been considered important key factors between inflammation and cancer [15]. Specifically, miRNA is a class of endogenous, small, noncoding RNAs that modulate gene expression by causing target mRNA degradation or inhibiting their translation [12,16]. Although miRNA short molecules are involved in complex pathways, specific miRNA signatures have been identified in a number of cancers, including laryngopharyngeal cancer [12,17,18]. Specifically, deregulation of "oncomirs" miR-21, -155, and -192 and tumor suppressors miR-375, -451a and -34a has been reported in laryngeal cancer [19–24]. Interestingly, an association was previously found between NF-κB activation and upregulation of oncogenic miR-21 and/or downregulation of tumor suppressors miR-34a and miR-451a [25,26], which are also deregulated in HNSCCs [12,19–22,24,27]. Moreover, GDF has been shown to stimulate the upregulation of specific biomarkers, like miR-192, in epithelial cells [28]. We hypothesize that the *in vivo* effect of GDF may deregulate oncogenic miRNAs in treated LM exhibiting significant NF-κB activation and histological and molecular alterations, supporting neoplastic transformation.

The hypopharynx and larynx are anatomically located at the junction of upper aero- and digestive tracts. Although the larynx is in close proximity to the hypopharynx, there is reason to suggest oncologic differences by quoted overall 5-year survivals. Supraglottic laryngeal cancer carries a 5-year survival of 43% versus hypopharyngeal cancer of 20% [29]. Furthermore, the supraglottic larynx differs from the glottic larynx (true vocal cords) in at least two ways: 1) the supraglottis consists of nonkeratinizing squamous epithelium and the vocal cords of stratified keratinizing squamous epithelium and 2) overall 5-year survivals of 43% versus 80%, respectively [29]. In this study, we will therefore limit our experimental inquiry to supraglottic rather than glottic tissue, the latter at greater risk to inhalant rather than digestive exposure.

Materials and Methods

In Vivo Mouse Model

We previously established an animal model to explore the effect of GDF in hypopharyngeal carcinogenesis via NF-κB activation [14]. Similar to our prior *in vivo* murine model, we established a mouse model using wild-type C57Bl/6J to study the effect of GDF on LM *in vivo*. As in that study, we used 35 wild-type C57B1/6J mice, shared in 4 experimental and 3 control groups (5 mice/group). Experimental fluids included 1) acidic bile salts, containing 10 mM of conjugated bile salts in a mixture (GCA + TCA + GCDCA + TCDCA + GDCA + TDCA; Sigma, St. Louis, MO, and Calbiochem, San Diego, CA) at molar concentration (20:3:15:3:6:1) as previously described [30], in buffered saline, brought to a pH of 3 with 1 M HCI (using a pH meter) and 2) neutral bile salts, containing the same bile salt mixture in buffered saline at pH 7.0. 3) DCA 10 mM, in buffered saline at pH 7.0 (Alfa Aesar, MA, USA) and 4) unconjugated chenodeoxycholic acid or CDCA 10 mM, in buffered saline at pH 7.0 (Sigma Aldrich, MO, USA). Control fluids consisted of 1) acid alone, consisting of buffered saline brought to pH 1.5 with 1 M HCI and considered as positive control; 2) highly concentrated glucose used as negative control (33 mM in buffered saline, pH 7.0); and 3) untreated control used as reference control.

pH 3.0 was selected because prior studies of 24-hour ambulatory pH monitoring in the pharynx of patients revealed frequent drops in pH to levels lower than pH 4.0 (excluding the influence of uncommon heterotopic gastric mucosa) [31]. We have used mixtures of conjugated bile acids at molar concentrations previously reported in symptomatic GERD patients [3]. In the case of DCA and CDCA, 10 mM test solutions were used in accordance with pharmacologic but nontoxic concentrations described in studies on rabbit esophagus [32], understanding that physiologic concentrations used in an *in vivo* model may be otherwise less effective.

We used a plastic feeding tube to administer a small quantity (150-200 μl) of experimental or control fluids to the larynx, twice a day for 45 days. At the end of experimental procedures, we harvested supraglottic laryngeal tissue from euthanized animals. These samples were obtained collectively from epiglottis, aryepiglotic folds, and false vocal cords from each animal. Four of five collective specimens were immersed immediately in 10% neutral buffered formalin and transported to the Pathology Department for paraffin embedding, whereas a fifth collective specimen was immersed in RNA stabilization solution (RNA*later*, Life Technologies) and kept in −20°C for molecular analysis.

Histological Analysis

Tissue sections of 3 to 4 μm from formalin-fixed and paraffin-embedded tissue specimens were stained with hematoxylin and eosin (H&E) for histological analysis. We examined H&E-stained slides by light microscopy, whereas images were captured and analyzed by Aperio CS2, Image Scope software (Leica Microsystems, Buffalo Grove, IL). Histopathological alterations were assessed according to previous criteria (WHO, Ljubljanska) [33,34] and laboratory mouse histology [35]. Normal mouse LM was characterized by intermediate epithelium (low squamoid epithelium) and was considered as controls. Hyperplasia was characterized by thickened intermediate epithelium. Abnormal hyperplasia was characterized by thickened intermediate epithelium with expansion of basal cells into the suprabasal layer without cytologic atypia, considered by some as a precursor for malignant transformation [33,34]. Thickness of epithelium was measured using the Aperio CS2, Image Scope software (Leica Microsystems). Mild-dysplastic epithelium was characterized by architectural disorder and/or hyperchromatic or pleomorphic basal cells expanded into the stratum spinosum but confined to the lower one third of the epithelium. Moderate dysplasia was demonstrated by nuclear hyperchromatism with a high degree of

basal layer expansion and/or nuclear hyperchromatism with increase of nuclear to cytoplasm ratios expanding into the middle third of the epithelium. Severe-dysplastic epithelium was characterized by marked full-thickness cytological changes including abnormal mitoses with loss of stratification. (All tissue specimens were grossly examined to exclude those with signs of local treatment toxicity, such as hemorrhagic lesions, ulceration, or inflammation).

Immunohistochemical Automated Quantified Analysis

We performed immunohistochemical analysis and automated quantified analysis (AQUA) to analyze the protein expression levels of p-NF-κB (p65 S536), Ki67, ΔNp63, CK14, E-cadherin, β-catenin, and p-STAT3 (Tyr705) in treated LM relative to untreated LM, as we previously described [14] (Supplementary methods).

Images of LM tissue sections were captured and analyzed using PM-2000 image workstation and HistoRX software. For each whole tissue section, areas of LM were selected, whereas compartments of submucosa were excluded, using AQUA software. The signal intensity of target antigen was acquired using DyLight 488 (similar to fluorescein isothiocyanate) signal or DYLight 549 (similar to Cy3) signal relative to tumor mask. The signal intensity of nuclei was acquired using DAPI signal. Maturing squamous cells that were losing their nuclei were counted as negative cells. AQUA scores within nucleus and cytoplasm (or membrane) were calculated by dividing the signal intensity by the area of the specified compartment.

miRNA Analysis

We performed miRNA analysis in murine GDF-treated LM and untreated controls to determine expression levels of miR-21, -155, -192, -375, -451a, and -34a previously characterized as laryngeal or hypopharyngeal cancer-related miRNAs [19–24,27]. We used miScript II RT kit (Qiagen, Louisville, KY) to perform reverse transcription synthesis of miRNAs from total RNA according to the manufacturer's instructions. Total RNA was isolated from representative murine laryngeal tissue specimens of GDF-treated groups (acidic bile, neutral bile, DCA, and CDCA) and of a normal untreated group using RNeasy mini kit (Qiagen). RNA quality and concentration ratios by absorption at 260 nm were determined using a NanoDrop 1000 spectrophotometer (Thermo Scientific). The quantification of specific miRNA markers was performed by quantitative polymerase chain reaction (qPCR) analysis (Bio-Rad real-time thermal cycler CFX96TM) using specific primers for target miRNAs of mouse genome (miScript Primer Assay, Qiagen) and normalization control small RNA RNU6B (snRNA RNU6-2; Qiagen) (Table 1), and miScript SYBR Green PCR Kit (Qiagen). Quantitative real-time PCR assays were performed in 96-well plates, and each sample was assayed in triplicate. These data were analyzed by CFX96TM software (Bio-Rad, Hercules, CA). Relative miRNA expression of experimental (acidic bile–, neutral bile–, DCA-, and CDCA-treated LM) to normal (untreated LM) was estimated by CFX96TM (Bio-Rad) software for each specific miRNA marker.

Table 1. Targets for Mouse Mature miRNA and RNU6 Small RNA Control, Analyzed by Real-Time qPCR, in Murine GDF-Treated LM and Untreated Control

miRNA (Mouse)	Target Mature miRNA
miR-21	mmu-miR-21a-5p, MI0000569
miR-192	mmu-miR-192-5p, MI0000551
miR-155	mmu-miR-155-5p, MI0000177
miR-375	mmu-miR-375-5p, MI0000792
miR-34a	mmu-miR-34a-5p, MI0000584
miR-451a	mmu-miR-451a, MI0001730
Small RNA	**Control**
RNU6-6P RNA, U6 small nuclear 6, pseudogene	Hs_RNU6-2_11

Statistical Analysis

We performed a statistical analysis using GraphPad Prism 6 software. Data obtained from AQUA and real-time qPCR analysis were calculated and analyzed by HistoRX (HistoRX Inc., Branford, CT) and CFX96TM (Bio-Rad) software, respectively. To obtain differences of AQUA scores, thickness of mucosa, or miRNA expression values between experimental and control groups, we performed comparisons using one-way analysis of variance (ANOVA), nonparametric Kruskal-Wallis test, and Holm-Sidak's or Dunn's multiple-comparison test (significance was defined as P values < .05). The correlation coefficient (r) between protein and miRNA expression levels of different groups was estimated *by* Pearson correlation (significance P values < .05).

Results

In Vivo GDF Induced Early Preneoplastic Alterations in Murine LM

The chronic exposure of GDF on murine LM, *in vivo*, induces early preneoplastic lesions [33,34,36–38] (Figure 1). Microscopic examination of H&E-stained and GDF-treated LM reveals hyperplastic and dysplastic changes compared with normal LM. In contrast, LM derived from mice exposed to acid alone or concentrated glucose produces no histologic change (Figure 1*A*). Specifically, hyperplasia of intermediate epithelium is identified in CDCA-treated LM (Figure 1*B*). Moreover, abnormal hyperplasia of intermediate epithelium and mild dysplastic changes are identified in neutral bile–treated LM (Figure 1*C*), whereas moderate dysplastic lesions are identified in acidic bile– and DCA-treated LM (Figure 1*D*). Neutral bile–, acidic bile–, and DCA-treated LM exhibits significant increase in thickness compared with normal untreated LM (2.1-3.8 × normal) or to LM exposed to acid alone (2.9-5.1 × acid) (P < .05; by Kruskal-Wallis) (Figure 1*E*). The graph in Figure 1*F* demonstrates the percentages of mice exhibiting histopathological alteration by treatment category. There are no histological signs of acute local treatment toxicity.

In Vivo GDF Induced NF-κB Activation and Correlations with Preneoplastic Alterations in LM

The microscopic examination of GDF-treated LM, and particularly at sites of hyperplastic or dysplastic lesions, reveals a significant activation of NF-κB (p65 S536) throughout its thickness (Figure 2) relative to normal (untreated LM) (Figure 2*A*). We find that neutral bile, acidic bile mixtures or bile components DCA or CDCA induce elevated NF-κB activation, indicated by an intense p-NF-κB nuclear staining of cells in basal extending to suprabasal layers (Figure 2*B*). In contrast, the untreated LM did not exhibit NF-κB activation by virtue of negative nuclear NF-κB (p65 S536) staining. Acid alone induces less intense and less extensive NF-κB activation compared with acidic bile (intense cytoplasmic p-NF-κB staining and few sporadic cells with nuclear p-NF-κB staining limited to the basal layer of LM). Finally, the glucose-treated LM exhibits low levels of NF-κB activation in few and sporadic cells, a pattern considered negative for NF-κB activation.

The immunofluorescence (IF) and AQUA analysis for NF-κB, cell proliferation markers, cell adhesion molecules, and STAT3 in

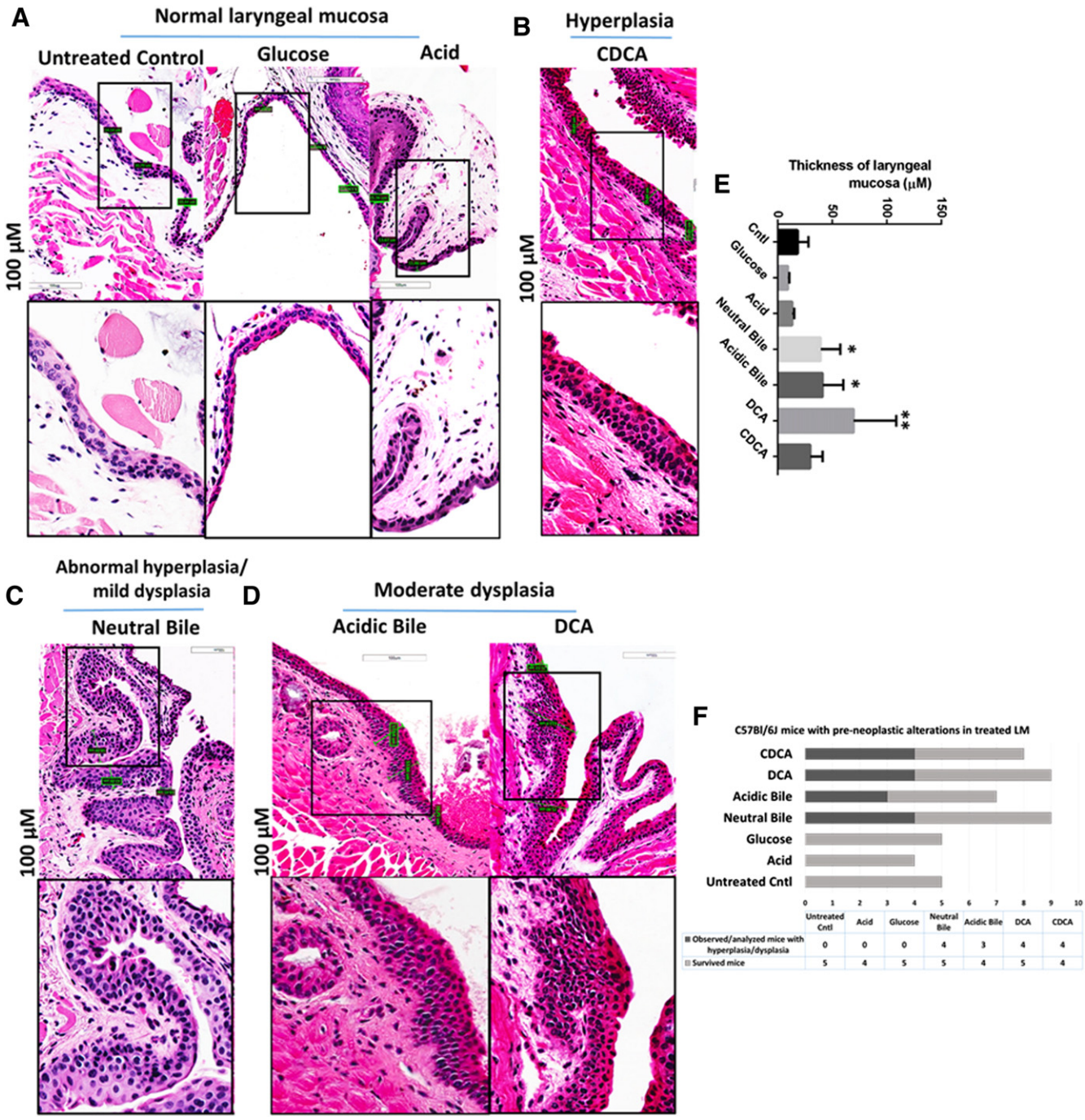

Figure 1. GDF-induced preneoplastic lesions in murine LM of C57BL/6J mice (H&E staining). (A) Normal LM: intermediate (low squamoid nonkeratinizing) epithelium. (B) Hyperplastic LM: thickened intermediate epithelium. (C) Abnormal hyperplastic/mildly dysplastic LM: thickened intermediate epithelium, hyperchromatic or pleomorphic basal cells expanding in the stratum spinosum. (D) Moderately dysplastic LM: high degree of basal layer expansion, nuclear hyperchromatism with increase of nuclear to cytoplasmic ratios, and loss of cell polarity. (E) Columns of graph created by GraphPad software correspond to mean thickness of LM under different treatments allowing comparison to control (*$P < .05$; **$P < .005$ ANOVA, Kruskal-Wallis test; GraphPad Prism 6.0). (F) Graph demonstrating the percentage of C57Bl/6J mice exhibiting histological alterations in LM.

GDF-treated LM compared with controls (Figure 3) reveals the following results:

A. *In Vivo* GDF Induces NF-κB and ΔNp63 Activation

The IF staining of p-NF-κB shown in Figure 3*A-a* confirms our results from chromogenic staining (Figure 2). Acidic bile–treated LM shows an intense and expanded nuclear p-NF-κB (p65 S536) (green) and ΔNp63 (red) staining in basal/parabasal and/or suprabasal layers, particularly at preneoplastic sites. Neutral bile–, DCA-, and CDCA-treated LM demonstrates nuclear p-NF-κB staining of basal/parabasal cells, particularly at hyperplastic or dysplastic sites, but with ΔNp63 staining expanding less in thickness than acidic bile–treated LM. Acid alone produces nuclear p-NF-κB staining in sporadic cells of basal/parabasal layers and ΔNp63 expression limited to the basal layer. In contrast, normal unteated LM exhibits a weak cytoplasmic p-NF-κB and nuclear ΔNp63 staining limited to the

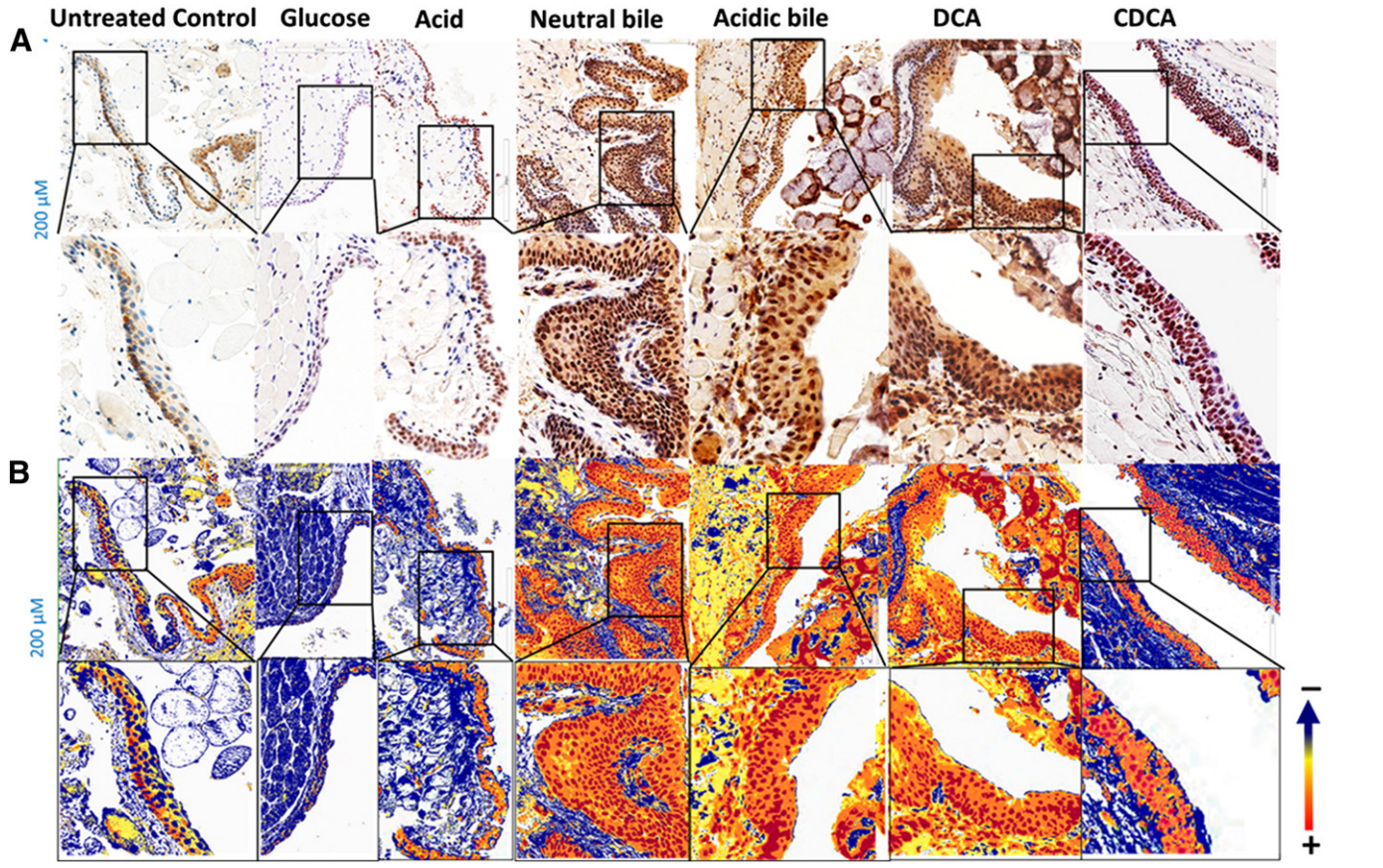

Figure 2. GDF-induced NF-κB activation in murine LM. (A) Immunohistochemical analysis for p-NF-κB (p65 S536) (from left to right): control (normal) untreated LM, cytoplasmic staining; glucose-treated LM, weak cytoplasmic or nuclear staining sporadically of few basal cells; acid alone–treated LM, nuclear or cytoplasmic staining mainly of cells of basal layer and weak cytoplasmic staining of suprabasal layers; hyperplastic/dysplastic neutral bile–, acidic bile–, DCA-, and CDCA-treated LM, intense nuclear and cytoplasmic staining of cells of basal and parabasal/suprabasal layers. (B) Image analysis algorithm(s) (red, nuclear positive staining of p-NF-κB; orange, intense positive cytoplasmic staining of p-NF-κB; yellow, weak cytoplasmic staining of p-NF-κB; blue, negative p-NF-κB staining). [Images were captured using Aperio CS2 and analyzed by Image Scope software (Leica Microsystems), which generated algorithm(s) illustrating the mucosal and cellular compartments demonstrating p-NF-κB staining].

basal layer, whereas glucose-treated LM exhibits similar staining found in normal untreated LM.

AQUA analysis reveals significantly higher nuclear p-NF-κB and ΔNp63 means of AQUA scores (AQUA-means) in the acidic bile–treated LM compared with untreated-LM ($P < .0005$ and $P < .005$, respectively) or compared with LM exposed to acid alone ($P < .005$), followed by neutral bile and CDCA compared with untreated LM ($P < .05$) (Figure 3*B-a*) (by Kruskal-Wallis).

B. *In Vivo* GDF Induces Increased Ki67 and Reduction of E-Cadherin

Acidic bile– and neutral bile–treated LM exhibits an expansion of Ki67 (green) expression, particularly at parabasal/suprabasal layers at preneoplastic sites, compared with normal untreated LM, acid alone–treated LM, or glucose-treated LM (Figure 3*A-b*). On the contrary, the same acidic bile– and neutral bile–treated LMs exhibit less intense E-cadherin (red) staining compared with normal untreated LM, acid alone–treated LM, or hyperplastic CDCA-treated LM exhibiting an intense E-cadherin staining within its entire thickness. Both DCA- and CDCA-treated LMs show Ki67 staining located at basal and/or parabasal layers.

AQUA analysis reveals significantly higher Ki67 AQUA-mean in the acidic bile–treated LM relative to normal untreated LM ($P < .05$) or compared with LM exposed to acid alone ($P < .0005$) (Figure 3*B-b*). AQUA-mean of Ki67 in neutral bile–, DCA-, and CDCA-treated LM is significantly higher compared with acid alone ($P < .005$, $P < .005$, and $P < .05$, respectively). Moreover, AQUA-mean of E-cadherin demonstrates significantly lower levels in the acidic bile– and neutral bile–treated LM versus untreated LM ($P < .05$) (Figure 3*B-b*) (by Kruskal-Wallis).

C. *In Vivo* GDF Induces Increased CK14 and β-Catenin Levels

We demonstrate in Figure 3*A-c* an extended CK14 (green) expression in the entire thickness of GDF-treated LM, and particularly in dysplastic acidic bile–treated LM, compared with normal untreated LM or acid alone–treated LM, in which CK14 is limited to the basal layer. Moreover, the same dysplastic acidic bile–treated LM and the hyperplastic CDCA-treated LM demonstrate an intense staining of β-catenin (red) compared with normal untreated LM or LM exposed to glucose or acid alone. AQUA analysis reveals a significant increase of CK14 and β-catenin AQUA-means in the acidic bile–treated LM relative to untreated LM ($P < .05$) or compared with LM exposed to acid alone ($P < .005$) (Figure 3*B-c*). We also show higher AQUA-mean of β-catenin in CDCA-treated LM versus untreated LM ($P < .05$) (Figure 3*B-c*) (by Kruskal-Wallis).

D. *In Vivo* GDF Induces STAT3 Activation

We demonstrate in Figure 3*A-d* an intense p-STAT3 (Tyr705) (green) nuclear staining in the GDF-treated LM and particularly in acidic bile–treated preneoplastic lesions. In contrast, the normal untreated LM shows no STAT3 activation, similar to LM exposed to glucose or acid alone. Neutral bile, DCA, and CDCA produces a weak p-STAT3 nuclear staining.

AQUA analysis reveals significantly higher nuclear p-STAT3 AQUA-mean in the acidic bile–treated LM compared with untreated LM ($P < .05$) (Figure 3*B-d*) (Kruskal-Wallis).

Correlations among p-NF-κB, Ki67, ΔNp63, CK14, β-Catenin, and E-Cadherin Molecular Alterations Induced by GDF

Pearson analysis reveals significant positive relationships among the underlying molecular alterations of GDF-treated LM (GraphPad Prism 6.0). Figure 4 demonstrates positive Pearson correlations between the expression levels (AQUA-means) of activated NF-κB and ΔNp63 ($r = 0.92418168$, $P = .0029$), p-STAT3 ($r = 0.950038572$, $P = .0010$), or

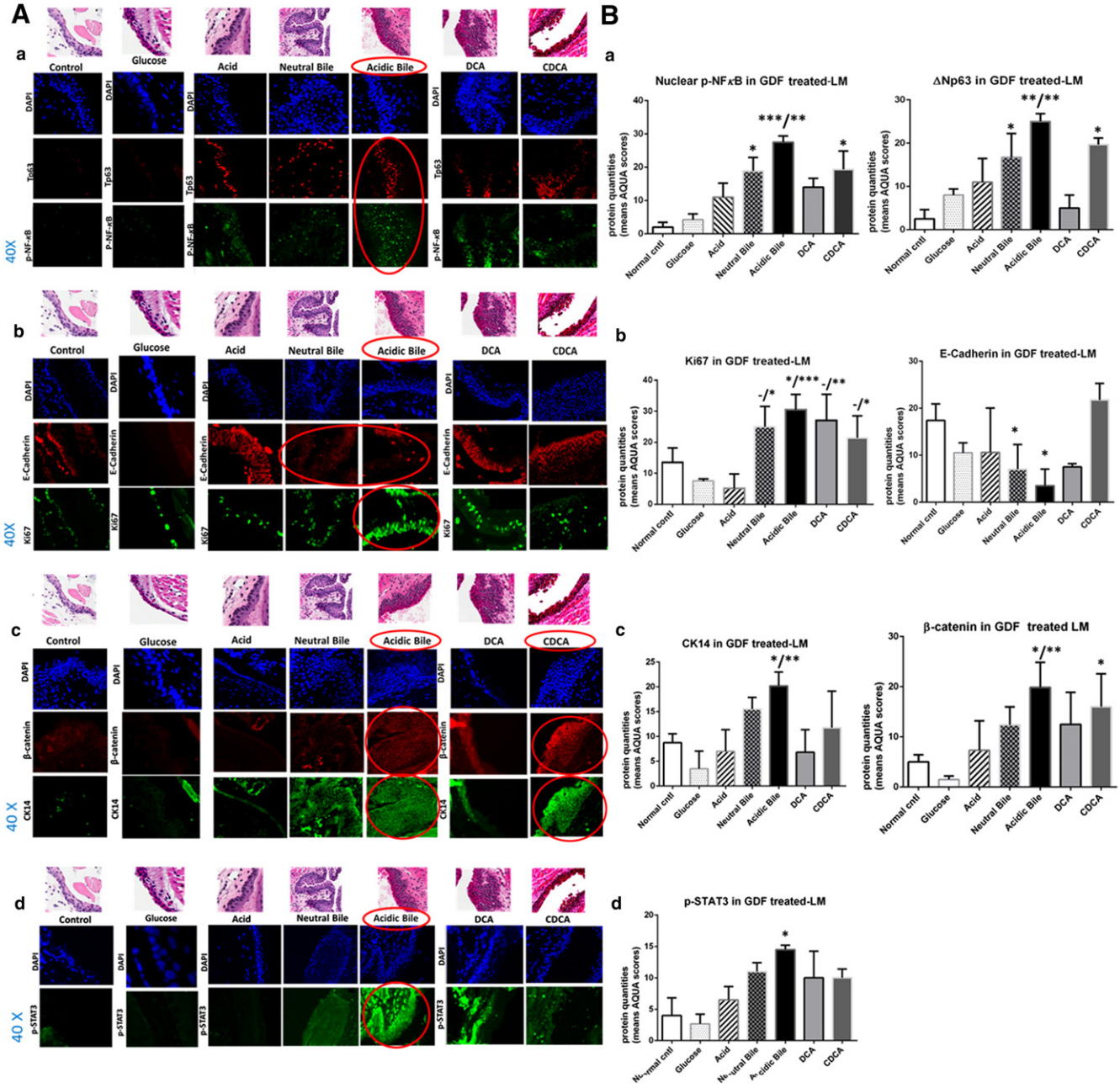

Figure 3. GDF induces molecular alterations underlying preneoplastic alterations of murine LM related to NF-κB activation, cell proliferation (indicated by increased ΔNp63, Ki67, and CK14 levels), EMT (supported by changes of cell-cell adhesion molecules E-cadherin and β-catenin), and STAT3 activation. IF staining (A) and AQUA (B) for (a) p-NF-κB (p65 S536) (green) and ΔNp63 (red); (b) Ki67 (green) and E-cadherin (red); (c) CK14 (green) and -catenin (red); and (d) p-STAT3 (Tyr705) (green) (from left to right): Normal untreated LM, glucose- and acid alone–treated LM; and hyperplastic/dysplastic neutral bile–, acidic bile–, DCA-, and CDCA-treated LM derived from C57Bl/6J mice. DAPI (blue) was used for nuclear staining (DyLight®488 for green and DyLight®549 for red). The box plots represent the mean ranks. The upper line indicates the highest value, the lower line the lowest value, and the middle line the mean of AQUA normalized quantities of each variable. Statistically significant difference between AQUA score means is indicated for GDF-treated LM versus normal untreated LM (right) and GDF- versus acid-treated LM (left) (*$P < .05$; **$P < .005$; ***$P < .0005$; one-way ANOVA, Kruskal-Wallis and Dunn's multiple comparison tests; GraphPad Prism 6.0).

β-catenin ($r = 0.883315706$, $P = .0084$) (Figure 4*A-a* and *b*), as well as between ΔNp63 and CK14 ($r = 0.905020427$, $P = .0051$) or p-STAT3 ($r = 0.900191778$, $P = .0057$) (Figure 4*A-c*), and between p-STAT3 and β-catenin ($r = 0.811874255$, $P = .0266$) (Figure 4*A-d*), and an inverse correlation between E-cadherin and β-catenin in GDF-treated LM ($r = -0.511020934$), particularly with respect to acidic bile–treated LM versus untreated LM ($r = -1$, $P < .0001$) (Figure 4*B*).

Acidic Bile Induced Deregulation of Cancer-Related miRNAs in LM

The *in vivo* effect of acid and bile combination on murine LM selectively induces deregulation of cancer-related miR-21, -155, -192, and -375 (Figure 5). Our miRNA analysis, by real-time qPCR, reveals a significant overexpression (upregulation) of "oncomirs" miR-21, -192, and -155 (Figure 5*A*) and a significant reduction (downregulation) of

tumor suppressor miR-375 (Figure 5*B*) in acidic bile–treated LM compared with untreated LM ($P < .0001$). In contrast, we observe an inverted phenotype for the analyzed miRNA markers in neutral bile– and DCA-treated LM, showing low or reduced levels of "oncomirs," particularly of miR-155 in neutral bile–treated LM compared with untreated LM ($P = .0123$), as well as increased levels of tumor suppressor miR-375 compared with untreated LM ($P = .0018$, and $P < .0001$, respectively). In the same way, the CDCA-treated LM produces an inverted phenotype for the analyzed "oncomirs," showing a significant reduction of miR-155 compared with untreated LM ($P = .0313$). However, we show that CDCA results in a significant reduction of tumor suppressor miR-375 in treated LM compared with untreated LM ($P < .0001$), similar to acidic bile. Moreover, our analysis shows that GDF, and particularly acidic bile, induces a significant reduction of tumor suppressor miR-34a and -451a in treated LM compared with untreated LM ($P < .0001$) (Figure 5*B*) (by one-way ANOVA; Holm-Sidak's multiple-comparisons test).

Our statistical analysis reveals that acidic bile induces the most significant deregulation (upregulation or downregulation) for the analyzed "oncomirs" and tumor suppressor miRNA markers compared with neutral bile ($P < .0001$ and $P = .0217$, respectively), DCA ($P = .0177$ and $P = .0038$, respectively), and CDCA ($P = .0020$) (Figure 5*C*) (by Kruskal-Wallis; Dunn's multiple-comparisons test).

Correlations among miRNA Deregulations in GDF-Affected Murine LM and between NF-κB Activation and Oncogenic miRNA Deregulation in Acidic Bile–Treated Murine LM

Pearson analysis reveals strong linear correlations among "oncomirs" expression in GDF-treated LM (Figure 6*A*). Specifically, we identify a significant positive correlation between miR-21 and -155 ($r = 0.997509461$) or miR-192 ($r = 0.99990467$) (Figure 6*A-a*) and between miR-155 and miR-192 ($r = 0.998075336$) ($P < .0001$) (Figure 6*A-b*).

Our analysis also reveals significant relationships between NF-κB activation and deregulation of oncogenic miRNA markers in acidic bile–treated LM. Specifically, we observe a strongly positive correlation between NF-κB activation and upregulation of "oncomirs" miR-21, -155, or -192 ($r = 1$, $P < .0001$) (Figure 6*B*). In contrast, we identify a strong inverted correlation between NF-κB activation and downregulation of tumor suppressor miR-34a, -451a, and -375 ($r = -1$, $P < .0001$) (Figure 6*C-a* and *b*).

Discussion

Although there have been efforts to link the effect of pepsin found in gastroesophageal refluxate to preneoplastic events in larynx and pharynx, the conclusions have been at best divergent. Adams favors the preneoplastic role of combined pepsin and acid [39], whereas Bock and Johnston defend the effect of nonacidic pepsin [40,41]. On the other hand, Del Negro in an *in vivo* rat model describes no evidence of neoplastic activity with pepsin and acid [42].

We chose to explore these events with respect to bile rather than pepsin in early neoplasia of laryngeal squamous epithelium. In this regard, we recently showed the tumorigenic effect of GDF on murine HM, mediated through the NF-κB–activated pathway, using a novel model of wild-type C57Bl6J mice [14]. Here we provide evidence that GDF induces preneoplastic transformation in murine LM related to and correlated with underlying molecular alterations through NF-κB activation and miRNA deregulation.

Various studies have proven that ΔNp63 is an oncogene linked to HNSCCs [43] and predictive of malignant transformation in oral

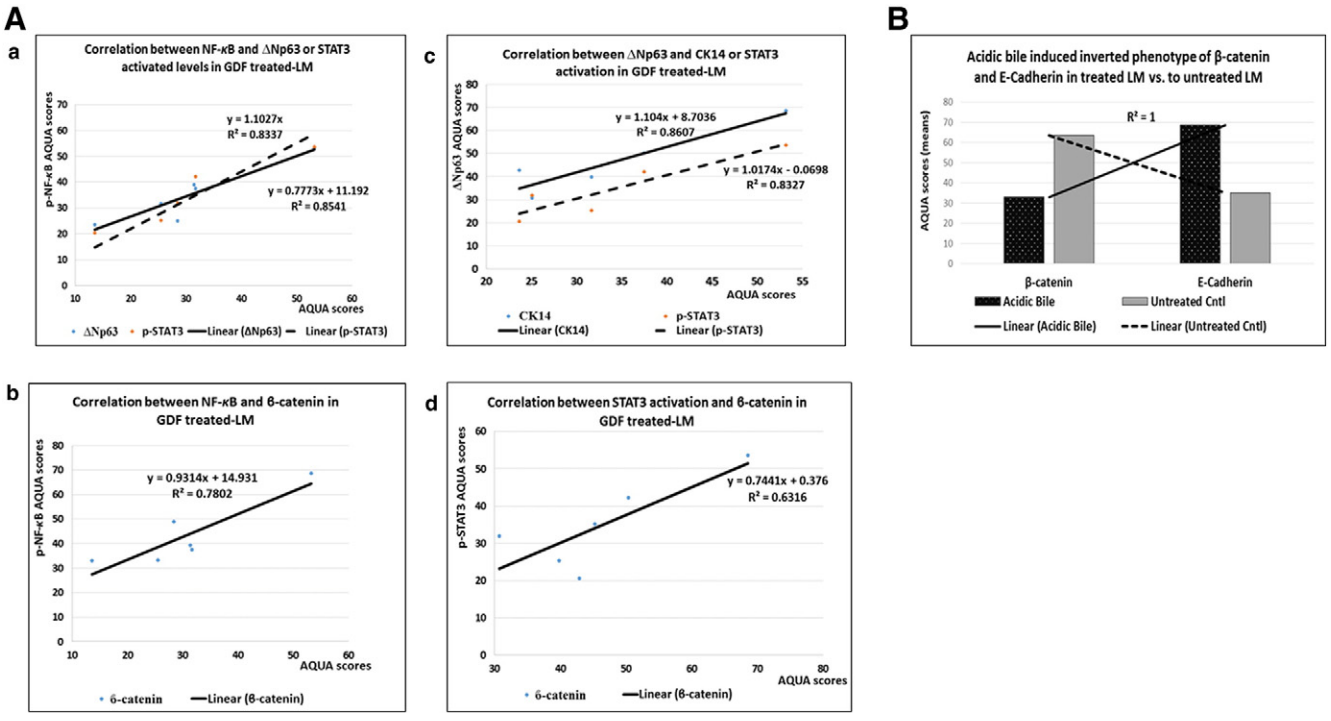

Figure 4. Correlation among GDF-induced molecular alterations in treated LM by Pearson. (A) Diagrams depicting positive correlation between (a) NF-κB and ΔNp63 or p-STAT3, (b) NF-κB and β-catenin levels, (c) ΔNp63 and CK14 or p-STAT3 levels, and (d) p-STAT3 and β-catenin levels in treated LM (P value < .05). (B) Graph demonstrates strong inverted phenotype of cell adhesion molecules β-catenin and E-cadherin in acidic bile–treated LM versus untreated LM (P value < .0001).

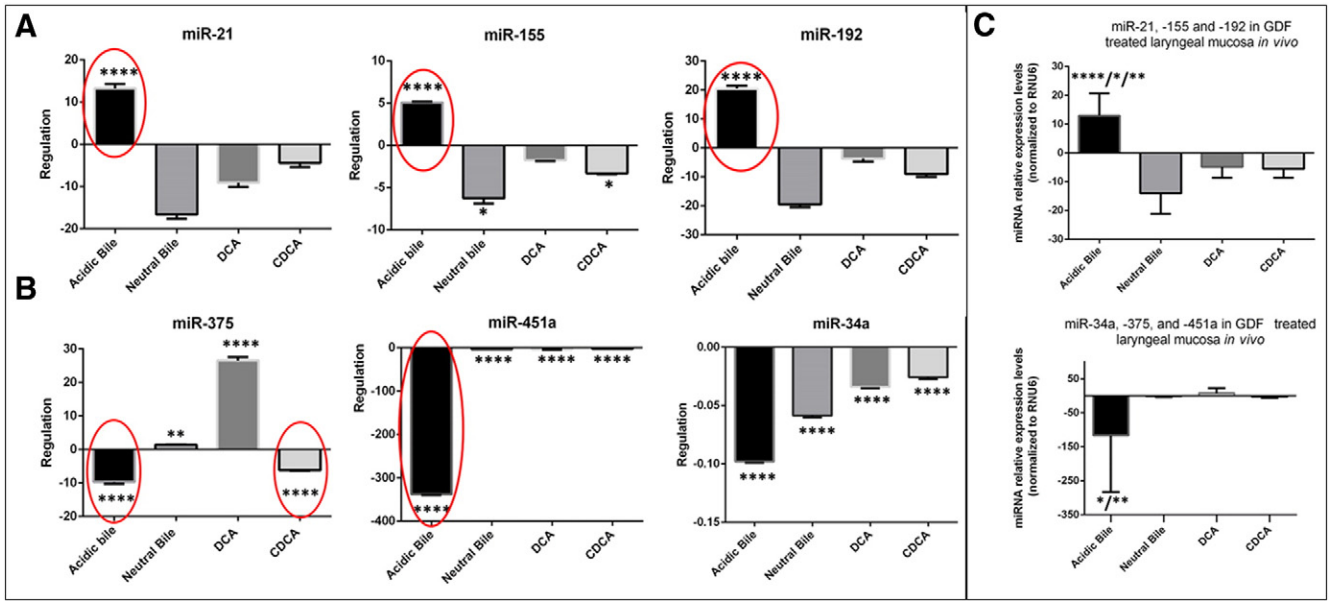

Figure 5. *In vivo* acidic bile induced deregulation of cancer-related miRNAs in murine LM. (A) Upregulation of "oncomirs" miR-21, miR-155, and miR-192 in acidic bile–treated LM versus untreated LM (by one-way ANOVA). (B) Downregulation of tumor suppressors miR-375, -34a, and -451a in GDF and particularly in acidic bile–treated LM versus untreated LM (by one-way ANOVA). (C) Graphs represent the deregulation of the analyzed "oncomirs" and tumor suppressor miRNAs in each GDF group of treatment. We show a significantly higher upregulation of "oncomirs" and more intense downregulation of tumor suppressor miRNAs in acidic bile–treated LM compared with LM exposed to neutral bile/DCA/CDCA (ANOVA, by Kruskal-Wallis). Columns of graphs created by Graph Pad Prism software 6.0 correspond to miRNA means. The upper line of column indicates the highest measurement (*$P < .05$; **$P < .005$; ***$P < .0005$;****$P < .00005$).

epithelial dysplasia and early stages of laryngeal tumorigenesis [44,45]. Our current data demonstrate that ΔNp63 is a major index of GDF-induced tumorigenic potential that appears specifically related to acid and bile salt combinations via NF-κB, in agreement with our prior *in vitro* data from human hypopharyngeal normal keratinocytes and *in vivo* findings from HM [13,14] and with previous studies

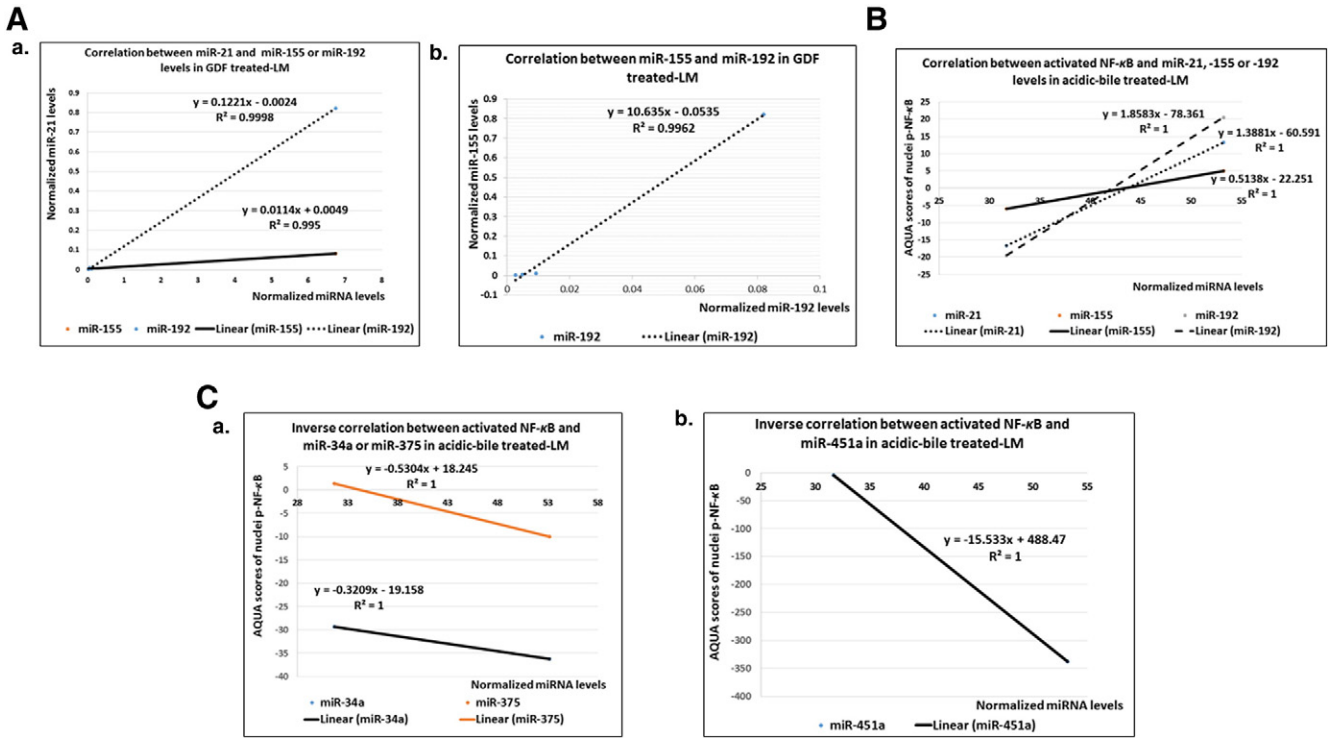

Figure 6. Correlation among GDF-induced deregulation of cancer related miRNAs and NF-κB activation. Diagrams depicting (A) positive correlation between (a) miR-21, -155, and -192 and (b) between miR-155 and -192 levels (miRNA levels normalized to RNU6); (B) positive correlation between NF-κB activation and "oncomirs" miR-21, -155, and -192 expression; and (C) an inverse correlation between acidic bile–induced NF-κB activation and tumor suppressors (a) miR-34a, miR-375, and (b) miR-451a expression in treated LM (*P* value < .0001; by Pearson).

supporting the ΔNp63/NF-κB interaction in cell proliferation processes of epithelial cells [46].

Increased expression of Ki67 and CK14, cell proliferation markers, previously identified in human laryngeal hyperplastic or dysplastic lesions [47,48] is considered to characterize early preneoplastic alterations of the upper aerodigestive tract [49]. Our data show that GDF-treated LM exhibits elevated and expanded expression of Ki67 and CK14, particularly at preneoplastic sites affected by acidic bile, indicating increased cell proliferation rates.

Significant changes in cell-cell adhesion molecules, such as β-catenin and E-cadherin, are previously linked to oral dysplastic lesions [50] and are related to malignant transformation of laryngeal tissues [51]. According to our prior *in vivo* findings, GDF-induced alterations of β-catenin and E-cadherin are also related to premalignant lesions in HM [14]. Our current data support an understanding that GDF-induced alterations of tight cell adhesions in treated LM may lead to a more mobile and a loosely mesenchymal phenotype previously identified as precursor to cancer linked to NF-κB activation [50,52]. Our current *in vivo* model demonstrates a significant inverted expression between E-cadherin and β-catenin proteins and between preneoplastic acidic bile–treated LM and normal untreated LM, supporting an EMT process, again in agreement with our prior study on HM [17].

Constitutive activation of signal transducers and activators of transcription, STAT3, has been linked to laryngeal carcinoma [53] and considered as an early event in head and neck carcinogenesis [54]. Our prior *in vitro* and *in vivo* models demonstrated that STAT3 activation linked to acidic bile induced NF-κB and a hypopharyngeal cancer-related phenotype. Our current model further demonstrates the acid and bile combination as related to STAT3 activation in LM compared with normal untreated LM or LM exposed to other stress factors such as glucose. We also confirm a linear correlation between STAT3 and NF-κB activation, in accordance with our prior findings in HM and other studies [14,55].

The selective effect of acidic bile on LM is further reflected by the significant deregulation of miRNA biomarkers, previously linked to laryngeal cancer [19–23]. Specifically, acidic bile but not neutral bile, DCA, or CDCA results in upregulation of "oncomirs" miR-21,-155, and -192 and down-regulation of tumor suppressor miR-375. Acidic bile also affects tumor suppressors miR-34a and -451a. Our findings are consistent with recent studies suggesting miR-21, miR-375, and miR-34a as risk factors of laryngeal carcinoma [20,24] and miR-451a as an important biomarker in hypopharyngeal carcinogenesis, linked to GDF [30], in accordance with Hu et al, who recently demonstrated miR-21/miR-375 ratio as an independent prognostic factor in laryngeal squamous carcinoma [21]. We assert that GDF affects LM by inducing a significant activation of NF-κB that may interact with specific miRNA molecules, supporting further cross talk between GDF stimulus response and tumorigenic processes.

Taken together, our data support the observation that GDF induces NF-κB activation at both low and neutral pH, although it appears that the differential effect at low pH (acidic bile) is more prominent than that at neutral pH (DCA and CDCA) at pharmacologic but nontoxic concentrations of 10 mM. However, at the same time, it is also very likely that DCA and CDCA at physiologic concentrations (0-282 μM) [4] may be constitutively ineffective. With respect to miRNA activation, there is clear predominance at low pH (acidic bile) as opposed to neutral pH (bile, DCA, CDCA).

Our model provides a mechanistic link and perhaps a new dimensional appreciation supporting the clinical observation often associating GERD, gastroduodenal reflux, and laryngeal neoplasia. Although *in vivo* models may not always correlate with patient-related conditions, the reduced effects of bile salts at neutral pH versus acidic bile enable us to suggest that the latter may be specifically injurious. One may also suggest that pharmacologic acid reduction in the presence of gastroduodenal reflux may at least partially impart a protective role. It is our hope of extending this model to investigate the effects of pepsin, alcohol, and tobacco on GDF-exposed LM and to determine the effects of NF-κB inhibition on tumor prevention and risk reduction in control of neoplastic recurrences.

Supplementary data to this article can be found online at http://dx.doi.org/10.1016/j.neo.2016.04.007.

Acknowledgements

This study was supported in part by an Ohse Award of Yale School of Medicine and by the Virginia Alden Wright Fund.

References

[1] El-Serag HB, Sweet S, Winchester CC, and Dent J (2014). Update on the epidemiology of gastro-oesophageal reflux disease: a systematic review. *Gut* **63**(6), 871–880.

[2] Sandler RS, Everhart JE, Donowitz M, Sandler RS, Everhart JE, Donowitz M, Adams E, Cronin K, Goodman C, and Gemmen E, et al (2002). The burden of selected digestive diseases in the United States. *Gastroenterology* **122**(5), 1500–1511.

[3] McQuaid KR, Laine L, Fennerty MB, Souza R, and Spechler SJ (2011). Systematic review: the role of bile acids in the pathogenesis of gastro-oesophageal reflux disease and related neoplasia. *Aliment Pharmacol Ther* **34**, 146–165.

[4] Nehra D, Howell P, Williams CP, Pye JK, and Beynon J (1999). Toxic bile acids in gastro-oesophageal reflux disease: influence of gastric acidity. *Gut* **44**, 598–602.

[5] Covington MF, Krupinski E, Avery RJ, and Kuo PH (2014). Classification schema of symptomatic enterogastric reflux utilizing sincalide augmentation on hepatobiliary scintigraphy. *J Nucl Med Technol* **42**(3), 198–202.

[6] Sweet MP, Patti MG, Hoopes C, Hays SR, and Golden JA (2009). Gastro-oesophageal reflux and aspiration in patients with advanced lung disease. *Thorax* **64**, 167–173.

[7] Koufman JA (1991). The otolaryngologic manifestations of gastroesophageal reflux disease (GERD): a clinical investigation of 225 patients using ambulatory 24-hour pH monitoring and an experimental investigation of the role of acid and pepsin in the development of laryngeal injury. *Laryngoscope* **101**(4 Pt 2 Suppl. 53), 1–78.

[8] Galli J, Cammarota G, Calò L, Agostino S, D'Ugo D, Cianci R, and Almadori G (2002). The role of acid and alkaline reflux in laryngeal squamous cell carcinoma. *Laryngoscope* **112**(10), 1861–1865.

[9] Wight R, Paleri V, and Arullendran P (2003). Current theories for the development of nonsmoking and nondrinking laryngeal carcinoma. *Curr Opin Otolaryngol Head Neck Surg* **11**(2), 73–77.

[10] Karin M (2006). Nuclear factor-kappaB in cancer development and progression (review). *Nature* **441**(7092), 431–436.

[11] Klein JD and Grandis JR (2010). The molecular pathogenesis of head and neck cancer. *Cancer Biol Ther* **9**(1), 1–7.

[12] Yan B, Li H, Yang X, Shao J, Jang M, Guan D, Zou S, Van Waes C, Chen Z, and Zhan M (2013). Unraveling regulatory programs for NF-kappaB, p53 and microRNAs in head and neck squamous cell carcinoma. *PLoS One* **8**(9), e73656.

[13] Sasaki CT, Issaeva N, and Vageli DP (2015). In vitro model for gastroduodenal reflux-induced nuclear factor-kappaB activation and its role in hypopharyngeal carcinogenesis. *Head Neck*. http://dx.doi.org/10.1002/hed.24231.

[14] Vageli DP, Prasad ML, and Sasaki CT (2016). Gastro-duodenal fluid induced Nuclear Factor-κappaB activation and early pre-malignant alterations in murine hypopharyngeal mucosa. *Oncotarget*. http://dx.doi.org/10.18632/oncotarget.6824.

[15] Tili E, Michaille JJ, and Croce CM (2013). MicroRNAs play a central role in molecular dysfunctions linking inflammation with cancer. *Immunol Rev* **253**(1), 167–184.

[16] Tong L, Yuan Y, and Wu S (2015). Therapeutic microRNAs targeting the NF-kappa B signaling circuits of cancers. *Adv Drug Deliv Rev* **81C**, 1–15.

[17] Calin GA and Croce CM (2006). MicroRNA signatures in human cancers. *Nat Rev Cancer* **6**(11), 857–866.

[18] Hui AB, Lenarduzzi M, Krushel T, Waldron L, Pintilie M, Shi W, Perez-Ordonez B, Jurisica I, O'Sullivan B, and Waldron J, et al (2010). Comprehensive MicroRNA profiling for head and neck squamous cell carcinomas. *Clin Cancer Res* **16**(4), 1129–1139.

[19] Zhou P, Zeng F, Liu J, Lv D, and Liu S (2015). Correlation between mir-21 expression and laryngeal carcinoma risks. *J Evid Based Med*. http://dx.doi.org/10.1111/jebm.12184.

[20] Hu A, Huang JJ, Xu WH, Jin XJ, Li JP, Tang YJ, Huang XF, Cui HJ, and Sun GB (2014). miR-21 and miR-375 microRNAs as candidate diagnostic biomarkers in squamous cell carcinoma of the larynx: association with patient survival. *Am J Transl Res* **6**(5), 604–613.

[21] Hu A, Huang JJ, Xu WH, Jin XJ, Li JP, Tang YJ, Huang XF, Cui HJ, Sun GB, and Li RL, et al (2015). MiR-21/miR-375 ratio is an independent prognostic factor in patients with laryngeal squamous cell carcinoma. *Am J Cancer Res* **5**(5), 1775–1785.

[22] Tai J, Xiao X, Huang ZG, Yu ZK, Chen XH, Zhou WG, Chen XJ, Rao YS, Fang JG, and Ni X (2013). MicroRNAs regulate epithelial-mesenchymal transition of supraglottic laryngeal cancer. *Zhonghua Er Bi Yan Hou Tou Jing Wai Ke Za Zhi* **48**(6), 499–503.

[23] Zhao XD, Zhang W, Liang HJ, Liang HJ, and Ji WY (2013). Overexpression of miR-155 promotes proliferation and invasion of human laryngeal squamous cell carcinoma via targeting SOCS1 and STAT3. *PLoS One* **8**(2), e56395.

[24] Shen Z, Zhan G, Ye D, Ren Y, Cheng L, Wu Z, and Guo J (2010). MicroRNA-34a affects the occurrence of laryngeal squamous cell carcinoma by targeting the antiapoptotic gene survivin. *Med Oncol* **29**(4), 2473–2480.

[25] Li J, Wang K, Chen X, Meng H, Song M, Wang Y, Xu X, and Bai Y (2012). Transcriptional activation of microRNA-34a by NF-kappa B in human esophageal cancer cells. *BMC Mol Biol* **13**, 4.

[26] Li HP, Zeng XC, Zhang B, Long JT, Zhou B, Tan GS, Zeng WX, Chen W, and Yang JY (2013). miR-451 inhibits cell proliferation in human hepatocellular carcinoma through direct suppression of IKK-β. *Carcinogenesis* **34**(11), 2443–2451.

[27] Fukumoto I, Kinoshita T, Hanazawa T, Kikkawa N, Chiyomaru T, Enokida H, Yamamoto N, Goto Y, Nishikawa R, and Nakagawa M, et al (2014). Identification of tumour suppressive microRNA-451a in hypopharyngeal squamous cell carcinoma based on microRNA expression signature. *Br J Cancer* **111**(2), 386–394.

[28] Bus P, Siersema PD, Verbeek RE, and van Baal JW (2014). Upregulation of miRNA-143, -145, -192, and -194 in esophageal epithelial cells upon acidic bile salt stimulation. *Dis Esophagus* **27**(6), 591–600.

[29] Freund HR (1967). The Principles of Head and Neck Surgery. New York: Appleton-Century-Crofts; 1967 .

[30] Kauer WK, Peters JH, DeMeester TR, Feussner H, Ireland AP, Stein HJ, and Siewert RJ (1997). Composition and concentration of bile acid reflux into the esophagus of patients with gastroesophageal reflux disease. *Surgery* **122**, 874–881.

[31] Sasaki CT and Toohill RJ (2000). 24 Hour Ambulatory pH Monitoring for Patients with Suspected Extraesophageal Complications of Gastroesophageal Reflux: Indications and Interpretations. *Ann Otol Rhinol Laryngol Suppl* **109**(10(2)), pp2.

[32] Farré R, van Malenstein H, De Vos R, Geboes K, Depoortere I, Vanden Berghe P, Fornari F, Blondeau K, Mertens V, and Tack J, et al (2008). Short exposure of oesophageal mucosa to bile acids, both in acidic and weakly acidic conditions, can impair mucosal integrity and provoke dilated intercellular spaces. *Gut* **57**(10), 1366–1374.

[33] Fleskens S and Slootweg P (2009). Grading systems in head and neck dysplasia: their prognostic value, weaknesses and utility (review). *Head Neck Oncol* **1**, 11.

[34] Gale N, Blagus R, El-Mofty SK, Helliwell T, Prasad ML, Sandison A, Volavšek M, Wenig BM, Zidar N, and Cardesa A (2014). Evaluation of a new grading system for laryngeal squamous intraepithelial lesions-a proposed unified classification. *Histopathology* **65**(4), 456–464.

[35] Claudio J. Conti, Irma B. Gimenez-Conti, Fernando Benavides, Anita F.W. Frijhoff and Mariano A. Conti. Reviewed by Jerrold M. Ward. Atlas of Laboratory Mouse Histology. Gastrointestinal. © 2004 Texas Histopages, Inc.

[36] Eversole LR (2009). Dysplasia of the upper aerodigestive tract squamous epithelium (review). *Head Neck Pathol* **3**(1), 63–68.

[37] Warnakulasuriya S, Reibel J, Bouquot J, and Dabelsteen E (2008). Oral epithelial dysplasia classification systems: predictive value, utility, weaknesses and scope for improvement. *J Oral Pathol Med* **37**(3), 127–133.

[38] Hellquist H, Lundgren J, and Olofsson J (1982). Hyperplasia, keratosis, dysplasia and carcinoma in situ of the vocal cords-a follow up study. *Clin Otolaryngol Allied Sci* **7**, 11–27.

[39] Adams J, Heintz P, Gross N, Andersen P, Everts E, Wax M, and Cohen J (2000). Acid/pepsin promotion of carcinogenesis in the hamster cheek pouch. *Arch Otolaryngol Head Neck Surg* **126**(3), 405–409.

[40] Bock JM, Howell AB, Johnston N, Kresty LA, and Lew D (2014). Upper esophageal and pharyngeal cancers. *Ann N Y Acad Sci* **1325**, 49–56.

[41] Johnston N, Yan JC, Hoekzema CR, Samuels TL, Stoner GD, Blumin JH, and Bock JM (2012). Pepsin promotes proliferation of laryngeal and pharyngeal epithelial cells. *Laryngoscope* **122**(6), 1317–1325.

[42] Del Negro A, Araújo MR, Tincani AJ, Meirelles L, Martins AS, and Andreollo NA (2008). Experimental carcinogenesis on the oropharyngeal mucosa of rats with hydrochloric acid, sodium nitrate and pepsin. *Acta Cir Bras* **23**(4), 337–342.

[43] Li X, Ottosson S, Wang S, Jernberg E, Boldrup L, Gu X, Nylander K, and Li A (2015). Wilms' tumor gene 1 regulates p63 and promotes cell proliferation in squamous cell carcinoma of the head and neck. *BMC Cancer* **15**, 342. http://dx.doi.org/10.1186/s12885-015-1356-0.

[44] Matsubara R, Kawano S, Kiyosue T, Goto Y, Hirano M, Jinno T, Toyoshima T, Kitamura R, Oobu K, and Nakamura S (2011). Increased ΔNp63 expression is predictive of malignant transformation in oral epithelial dysplasia and poor prognosis in oral squamous cell carcinoma. *Int J Oncol* **39**(6), 1391–1399.

[45] Re M, Zizzi A, Ferrante L, Stramazzotti D, Goteri G, Gioacchini FM, Olivieri F, Magliulo G, and Rubini C (2014). p63 and Ki-67 immunostainings in laryngeal squamous cell carcinoma are related to survival. *Eur Arch Otorhinolaryngol* **271**(6), 1641–1651.

[46] Lu H, Yang X, Duggal P, Allen CT, Yan B, Cohen J, Nottingham L, Romano RA, Sinha S, and King KE, et al (2011). TNF-α promotes c-REL/ΔNp63α interaction and TAp73 dissociation from key genes that mediate growth arrest and apoptosis in head and neck cancer. *Cancer Res* **71**, 6867–6877.

[47] Mondal D, Saha K, Datta C, Chatterjee U, and Sengupta A (2013). Ki67, p27 and p53 Expression in Squamous Epithelial Lesions of Larynx. *Indian J Otolaryngol Head Neck Surg* **65**(2), 126–133.

[48] Ueno T, Hoshii Y, Cui D, Kawano H, Gondo T, Takahashi M, and Ishihara T (2003). Immunohistochemical study of cytokeratins in amyloid deposits associated with squamous cell carcinoma and dysplasia in the oral cavity, pharynx and larynx. *Pathol Int* **53**(5), 265–269.

[49] Pereira CS, Oliveira MV, Fraga CA, Barros LO, Domingos PL, Roy A, De-Paula AM, and Guimarães AL (2012). Impact of the epithelial dysplasia grading and Ki67 proliferation index in the adjacent non-malignant mucosa on recurrence and survival in head and neck squamous cell carcinoma. *Pathol Res Pract* **208**, 651–656.

[50] Chaw SY, Majeed AA, Dalley AJ, Chan A, Stein S, and Farah CS (2012). Epithelial to mesenchymal transition (EMT) biomarkers-E-cadherin, beta-catenin, APC and Vimentinin oral squamous cell carcinogenesis and transformation. *Oral Oncol* **48**, 997–1006.

[51] López F, Alvarez-Marcos C, Alonso-Guervós M, Domínguez F, Suárez C, Hermsen MA, and Llorente JL (2013). From laryngeal epithelial precursor lesions to squamous carcinoma of the larynx: the role of cell cycle proteins and β-catenin. *Eur Arch Otorhinolaryngol* **270**(12), 3153–3162.

[52] Chung CH, Parker JS, Ely K, Carter J, Yi Y, Murphy BA, Ang KK, El-Naggar AK, Zanation AM, and Cmelak AJ, et al (2006). Gene expression profiles identify epithelial-to-mesenchymal transition and activation of nuclear factor-kappaB signaling as characteristics of a high-risk head and neck squamous cell carcinoma. *Cancer Res* **66**, 8210–8218.

[53] Goswami KK, Barik S, Banerjee S, Bhowmick AK, Biswas J, Bose A, and Baral R (2013). Supraglottic laryngeal tumor microenvironmental factors facilitate STAT3 dependent pro-tumorigenic switch in tumor associated macrophages to render utmost immune evasion. *Immunol Lett* **156**(1-2), 7–17.

[54] Grandis JR, Drenning SD, Zeng Q, Watkins SC, Melhem MF, Endo S, Johnson DE, Huang L, He Y, and Kim JD (2000). Constitutive activation of Stat3 signaling abrogates apoptosis in squamous cell carcinogenesis in vivo. *Proc Natl Acad Sci U S A* **97**(8), 4227–4232.

[55] Squarize CH, Castilho RM, Sriuranpong V, Pinto Jr DS, and Gutkind JS (2006). Molecular cross-talk between the NFkappaB and STAT3 signaling pathways in head and neck squamous cell carcinoma. *Neoplasia* **8**, 733–746.